Subject-specific multi-rx data combination using two-stage optimization for phase-based EPT

Jaewook Shin[1], Joonsung Lee[2,3], Min-oh Kim[1], Narae Choi[1], and Dong-Hyun Kim[1]
[1]*Department of Electrical and Electronic Engineering, Yonsei University, Seodaemun-Gu, Seoul, Korea,* [2]*SIRIC, Yonsei University, Seodaemun-Gu, Seoul, Korea,*
[3]*Nanomedical Research Center, Yonsei University, Seoul, Korea*

***Purpose*:** Phase-based EPT is to estimate in-vivo conductivity distribution using only B_1 phase information. In phase-based EPT, the accuracy of estimated conductivity values relies on the spatial variation of the magnitude of transmit ($|B_1^+|$) [1]. In addition, using a multi-receive coil (multi-Rx), the spatial variation of combined B_1^- magnitude should be negligible for phase-based EPT [2,3]. Previously, pre-calibrated by phantom experiments, a method for multi-Rx data combination was introduced [2]. In this study, we propose subject-specific data combination methods shown in Fig. 1 based on a mask generation over a globally distributed tissue and two-stage magnitude least square (MLS) optimization [4] to reduce the spatial variation of combined B_1^- magnitude. Phantom and in-vivo experiments were performed at 3T.

Method: The magnitude of MR image can be simplified as $|I(r)| = C(r)f(|B_1^+(r)|)|B_1^-(r)|$ where $C(r)$ is a tissue contrast, $f(\cdot)$ is an excitation profile and $|B_1^-(r)|$ is a magnitude of receive profile. Using quadrature body coil (QBC) as a transmit coil at 3T for brain imaging, we assumed $|B_1^+(r)|$ was sufficiently homogeneous [5]. Additionally, we assumed tissue contrast was homogeneous for a specific tissue. With these assumptions, the spatial variation of the image is mainly dependent on $|B_1^-(r)|$. To find a data combination method that homogenizes combined $|B_1^-|$, we found a region of globally distributed tissue, selected the region as region of interest (ROI), and determined coefficients of linear combination of multi-Rx data that homogenize the combined magnitude image over ROI. ROI was generated using magnitude threshold based on a histogram for a globally distributed tissue.

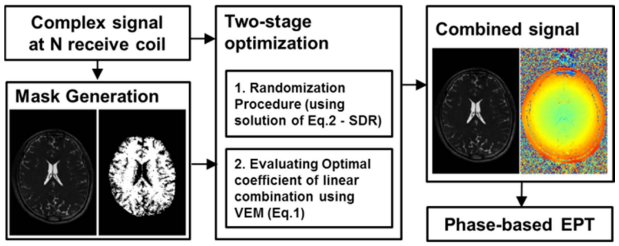

Fig 1 Flow diagram–The proposed conductivity reconstruction methods, multi-Rx data combined by two-stage optimization

Multi-Rx data combination: Let $I_p = [I_{p,1}, \cdots, I_{p,N_c}]^T \in \mathbb{C}^{N_c}$ be the complex images at each receive coils and N_c be the number of the receive coils. The vector $w \in \mathbb{C}^{N_c}$ denotes the coefficients of linear combination of multi-Rx data, where the linear combination can be expressed as $I_p w$. The coefficients, w, were determined to homogenize the magnitude of combined image I by solving Eq. 1.

$$w = \text{argmin}_w \left\{ \sum_{p=1}^{N_p} \left| |I_p^T w|^2 - 1 \right| \right\} \qquad (1)$$

Variable Exchange Method (VEM), which is iteratively tracing the solution from random initial point, [6] can be used to determine the coefficients. The performance of VEM method relies on initial point and VEM does not guarantee global minima. To find a better initial point and achieve global minima of Eq.1, Eq.1 was transformed to a Semi-Definite Relaxation (SDR) problem as Eq.2. [4]

$$W = \text{argmin}_{W=ww^T} \left\{ \sum_{p=1}^{N_p} \left| |I_p^* I_p^T W|^2 - 1 \right| \right\} \qquad (2)$$

The solution of Eq. 2, W, to achieve global minima can be determined. However, it is not sufficient to evaluate the vector w. Therefore, through randomization processing with N_r =200 in this study, a reliable initial point, w_0, was chosen and with the initial point VEM method was applied to determine the coefficients of linear combination, w, as shown in Fig. 1. To compare the performances, magnitude least square optimization using random initialization and SDR initialization was iteratively performed using experimental phantom data with 1,000 trials. For each initialization, normalized root mean square (NRMSE) and signal to noise ratio (SNR) of combined magnitude images were evaluated. Then, the distributions of NRMSE and SNR were demonstrated as histograms as shown in Fig. 2.

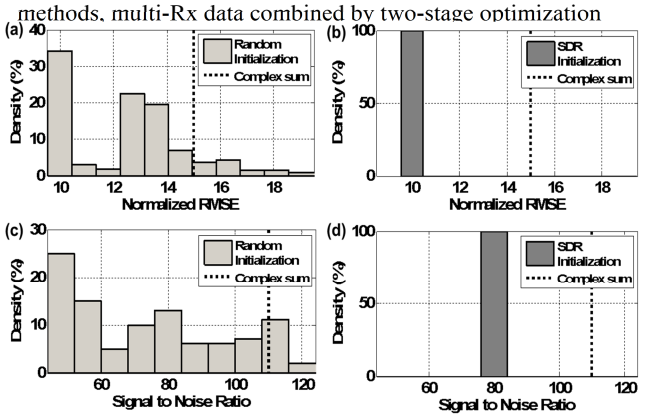

Fig 2 Histograms of NRMSE (a,b) and SNR (c,d) of combined image using optimization with random (left) and SDR (right) initialization

Phantom, In-vivo Experiments and Reconstructions: Phantom and in-vivo imaging were performed in a 3T clinical scanner (3T Siemens Tim Trio MRI scanner) with a 12-channel head coil using 3D TrueFISP sequence (Flip angle = 45°, TR/ TE≈4.8/2.4ms with 4 average) and 3D MPRAGE sequence (Flip angle = 9°, TR/TE/TI=2300/3/900ms) for voxel size = 1 × 1 × 1 mm^3. Total in-vivo scan time was about 15 min. From phase of multi-Rx combined 3D TrueFISP image, φ, conductivity map was reconstructed using $\sigma = (2\omega\mu_0)^{-1}\nabla^2\varphi$ where ω is larmor frequency and μ_0 is the magnetic permeability. To reduce noise amplification in calculating Laplacian operator, adaptive 3D weighted second-order fitting was applied. The weighting factors were locally evaluated using the magnitude image of 3D MPRAGE.

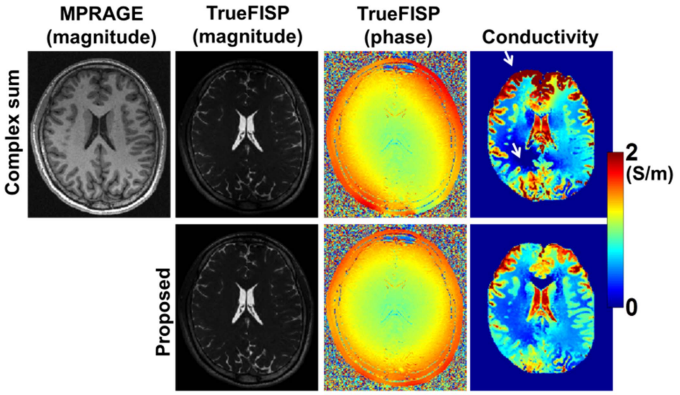

Fig 3 MPRAGE, TruFISP (magnitude, phase) and conductivity image (first row: coil combination using VEM with random initialization, second row: coil combination using VEM with SDR initialization)

Results & Conclusion: In our experiment, NRMSE values of combined images using random initialization was distributed from 10 % to 17 % but NRMSE values of combined images using SDR initialization was below 11%. (Fig. 2a, b) This result about the optimality of SDR initialization was almost correspond to the transmit B_1 shimming at 7T. [4] However, this minimization does not guarantee the optimal SNR as shown in Fig. 2c, d. Therefore, to enhance SNR of combined image, regularization term can be considered as [3]. In Fig. 3, the difference of combined images between complex sum and proposed method was much more visible in phase image than magnitude image. In addition, as shown in conductivity image in Fig. 3, the proposed methods reduce conductivity errors (white arrows) that may be produced by non-negligible spatial variation of B_1^- magnitude.

References: 1.Voigt et al, MRM(2011) 66:456–466 2.J Shin et al, ISMRM(2013) 4180 3.J Lee et al, ISMRM(2013) 4179 4.T-H chang et al. ISMRM (2008) 1088 5.Voigt et al, MRM(2012) 68:1117–1126 6.K. Setsompop et al, MRM (2008) 59:908–915